Near-infrared Fourier transform Raman, surface-enhanced Raman scattering and Fourier transform infrared spectra and ab initio calculations of the natural product nodakenetin angela...

ARTICLE *in* JOURNAL OF RAMAN SPECTROSCOPY · JANUARY 2005

Impact Factor: 2.67 · DOI: 10.1002/jrs.1272

JOURNAL OF RAMAN SPECTROSCOPY
J. Raman Spectrosc. 2005; **36**: 63–72
Published online 1 December 2004 in Wiley InterScience (www.interscience.wiley.com). DOI: 10.1002/jrs.1272

JRS

Near-infrared Fourier transform Raman, surface-enhanced Raman scattering and Fourier transform infrared spectra and *ab initio* calculations of the natural product nodakenetin angelate

J. Binoy,[1] Jose P. Abraham,[1] I. Hubert Joe,[1] V. George,[2] V. S. Jayakumar,[1]* J. Aubard[3] and O. Faurskov Nielsen[4]

[1] Department of Physics, Mar Ivanios College, Thiruvananthapuram - 695 015, Kerala, India
[2] TBGRI, Palode, Thiruvananthapuram, Kerala, India
[3] ITODYS, Université Paris VII, 1 rue Guy de la Brosse, 75005 Paris, France
[4] Department of Chemistry, University of Copenhagen, 5 Universitetsparken, DK-2100 Copenhagen, Denmark

Received 24 May 2004; Accepted 27 September 2004

Near-infrared Fourier transform Raman and Fourier transform infrared spectra of nodakenetin angelate ($C_{19}H_{20}O_5$), extracted from seeds of *Heracleum candolleaum*, were recorded and analysed. The root extract of this plant is used as an antiarthritic and nerve tonic. *Ab initio* SCF Hartree–Fock computations were performed employing the 6–31G basis set for geometry optimization for the prediction of IR and Raman spectral activities and wavenumber calculations. Parameters initially optimized using AM1 calculations were used as the input for *ab initio* computations. The computed results were used for the interpretation of the vibrational spectra. Important thermodynamic parameters were also provided. The strong band at 1712 cm^{-1} and medium-intensity band at 1731 cm^{-1} resulting from ester and lactone carbonyl vibrations, respectively, are identified in the Raman spectrum. The C═O stretching band in IR is broadened around 1717 cm^{-1} owing to the overlapping of ester and lactone carbonyl vibrations. The lowering of the carbonyl stretching vibrations is due to conjugation. The computed values indicate a larger degree of conjugation for the ester group. The characteristic vibrations of the furanocoumarin ring which is part of the molecule were identified. The CH stretching and bending vibrations of the CH_3 group of the ester part indicate the presence of hyperconjugation. Vibrational analysis indicates the presence of blue-shifting H-bonds resulting from interaction of the methyl group The large enhancement of in-plane ring stretching and ring breathing modes in the surface-enhanced Raman scattering spectrum indicates that the molecule is adsorbed on the silver surface in a 'vertical' configuration, with the lactone ring perpendicular to the silver surface and probably on the opposite side of the lactonic C═O group. Copyright © 2004 John Wiley & Sons, Ltd.

KEYWORDS: vibrational spectra; near-infrared Fourier transform Raman; infrared; *ab initio*; surface-enhanced Raman scattering; blue-shifting H-bonds

INTRODUCTION

Raman spectroscopy has recently been proved to be a valuable tool in the investigation of complex molecules of biological interest.[1–4] Being a non-destructive method, which requires micro quantities of samples, the Raman spectroscopy technique offers tremendous scope for the investigation of the molecular mechanics of rare biological samples available only in very small quantities. Surface-enhanced Raman scattering (SERS) spectroscopy is an increasingly important technique in studies of biomolecules adsorbed on a metal surface. Highly selective and sensitive SERS spectra give the vibrational fingerprint of adsorbed molecules. Owing to the high information content of these spectra, they are considered to be unique for studying the surface

*Correspondence to: V. S. Jayakumar, Department of Physics, Mar Ivanios College, Thiruvananthapuram - 695 015, Kerala, India.
E-mail: vsjk@vsnl.net

orientation and the mode of binding of adsorbed molecules on a metal surface. Although vibrational spectral studies of biomolecules and natural products extracted from plants can reveal the characteristic features of these molecules, very little work has been reported in such compounds. The non-availability of biological compounds of high purity in bulk quantities and fluorescence associated with conventional Raman spectra are the major difficulties in undertaking such investigations. The recent innovations in near-infrared Fourier transform (NIR-FT) Raman spectroscopic instrumentation have come as a promising tool for such investigations, which provides fluorescence-free Raman spectra. Recently, vibrational spectral investigations and theoretical computations related to the natural products columbianadin,[5] coumarin 152,[6] cresyl violet perchlorate,[6] ginkgolide[7] and combretastatin-A4[8] and compounds of biological interest[9] have attracted great interest owing to their importance in the medical field. As part of studies on the structural and bonding features of natural product molecules, we report here the vibrational spectra and computations relating to the natural product nodakenetin angelate (NKA) (Fig. 1), extracted from *Heracleum candolleanum*, an endemic plant, locally known as 'Vadamparathi'. The plant, found in the Western Ghat region of peninsular India at altitudes above 6000 ft,[10] is used by tribes of the region for various ailments such as nervous disorders and inflammatory conditions. The root extract of these plants is used as an antiarthritic agent and as a nerve tonics.[11]

NKA is a linear dihydrofuranocoumarin. Furanocoumarins in general are used as dermal photosensitizers (e.g. xanthotoxin, bergapten, imperatorin, angelicin) and hence they find use in the preparation of sun-tan lotions. Their useful physiological effect is due to their ability to sensitize mammalian skin to UV light. The coumarin derivatives absorb short-wavelength UV radiation (280–315 nm) that is harmful to skin, but transmit the long-wavelength UV radiation (315–400 nm) that gives a brown sun-tan.[12] NKA is present in 0.18% yield in the fruits of *Heracleum candolleanum* along with other furanocoumarins and hence the light petroleum extract of the fruits of *H. candolleanum* may find use in the preparation of sun-tan lotions, which is to be confirmed by detailed pharmacological and toxicological studies.

EXPERIMENTAL

Preparation

The seeds and roots of *H. candolleanum* were collected from the Munnar region of Western Ghat. Dried, powdered seeds (300 g) and roots (325 g) were extracted separately with hexane in a Soxhlet extractor and worked up in the usual manner to obtain 18 and 17 g of the extracts, respectively.

The hexane extract (15 g) from seeds was subjected to column chromatography on silica gel followed by medium-pressure liquid chromatography on silica gel with a gradient elution program, the eluent being 3–20% EtOAc in hexane. Work-up of the eluate fractions afforded 70 mg (yield 0.023%) of a colourless, silky, needle-shaped, pure crystalline substance from hexane–EtOAc, m.p. 100–101 °C. This compound was identified as nodakenetin angelate ($C_{19}H_{20}O_5$)[13,14] from IR, UV and ^{1}H and ^{13}C NMR data.

IR and Raman measurements

The Raman spectrum (Fig. 2) was obtained on a Bruker IFS66 NIR-FT instrument equipped with a FRA106 Raman module. An Nd : YAG laser at 1064 nm with an output of 300 mW was used for excitation. The detector was a Ge diode cooled to liquid nitrogen temperature. A total of 1000 scans were accumulated with a total registration time of about 30 min. The spectral resolution after apodization was 6 cm^{-1}. A correction according to the fourth-power scattering factor was performed, but no correction to instrumental response was applied. The upper limit for the wavenumbers

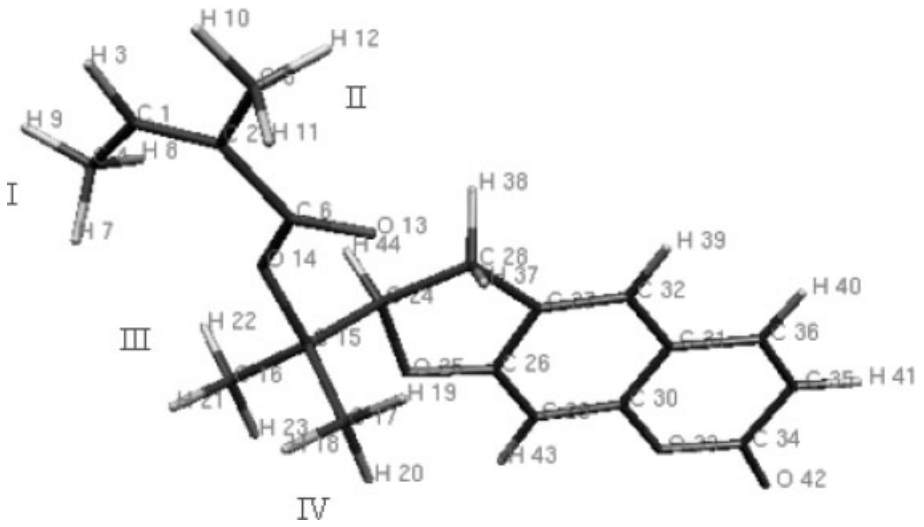

Figure 1. Structure of nodakenetin angelate optimized using Hartee–Fock calculation.

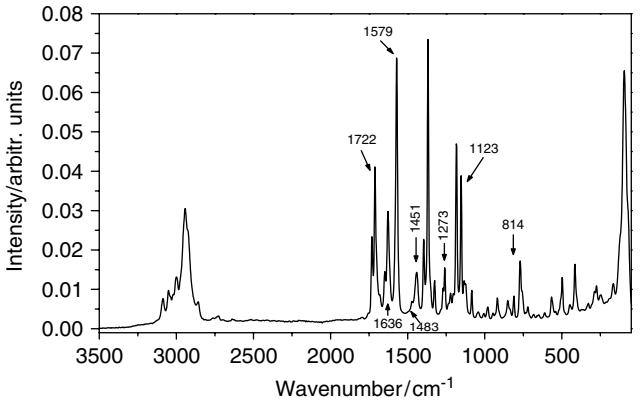

Figure 2. NIR-FT Raman spectrum of nodakenetin angelate in the solid state.

is 3500 cm^{-1} owing to the detector sensitivity and the lower wavenumber limit is around 85 cm^{-1} owing to the Rayleigh line cutoff by a notch filter.

The IR spectrum (Fig. 3) was recorded on a Perkin-Elmer FT-IR 1760X instrument. The spectral resolution was 4 cm^{-1}. The standard KBr technique with 1 mg of sample per 300 mg of KBr was used.

The SERS spectrum (Fig. 4) was recorded using a DILOR XY multichannel spectrometer with argon ion laser excitation at 514.5 nm using 30–40 mW power and a spectral resolution of 2 cm^{-1}. Silver colloids obtained by the Creighton method were used. A series of SERS experiments were conducted at different concentrations and under different conditions. It is found that in the concentration range 10^{-3}–10^{-5} M the SERS spectra display the same band position and relative intensity distribution irrespective of NKA concentration, ruling out the possibility of self-association. In this concentration range, no Raman spectrum was detected in the absence of Ag colloid, indicating that there is no contribution to the SERS signal from bulk solution. $NaNO_3$ (40 mM) was added just before

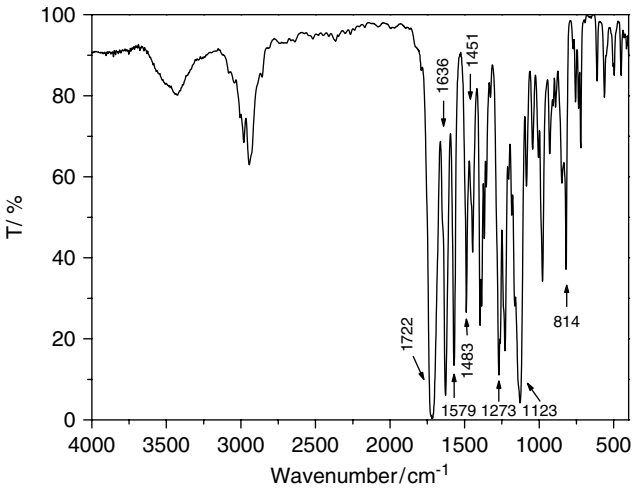

Figure 3. FT-IR spectrum of nodakenetin angelate.

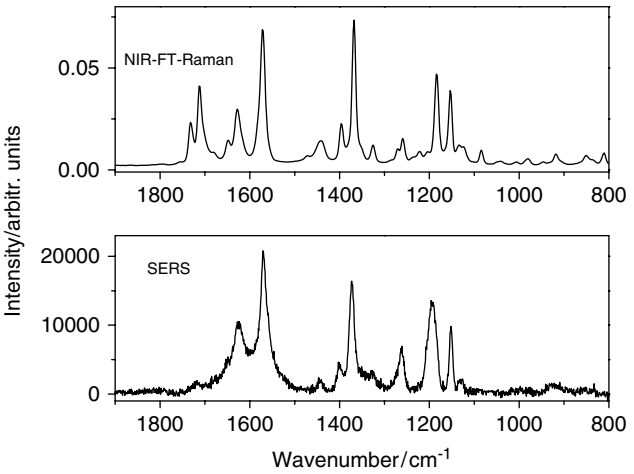

Figure 4. SERS spectrum (bottom) and NIR-FT Raman spectrum (top) of nodakenetin angelate shown in the same wavenumber region.

the spectrum was recorded, as an aggregating agent. The SERS spectral features were found to be similar with and without $NaNO_3$ salt, but a 100-folds intensity enhancement of the SERS signal was observed with the addition of $NaNO_3$.

Computational details

Ab initio computations on NKA were performed using the Gaussian 98 program package.[15] Parameters initially optimized using AM1 calculations were used as input for *ab initio* computations. Structures for the ester and lactone parts were first individually optimized at the HF/6–31G level; these structures were used as starting geometries to optimize the structure of NKA at the same level of theory (Table 1). All the molecular and intermolecular parameters defining the NKA were left free for optimization. The vibrational wavenumber calculation performed at the HF/6–31 G level was used to permit a detailed assignment of the spectral features of NKA (Table 2).

RESULTS AND DISCUSSION

Thermodynamic parameters

The calculated results revealed the following thermodynamic parameters: the self-consistent field (SCF) energy of NKA is −1104.9851 hartree, the zero-point vibrational energy is 1008.07 kJ mol^{-1}, the entropy is 598.43 J mol^{-1} and C_v is 316.75 J mol^{-1} K^{-1}.

Vibrational spectrum

The calculated vibrational spectrum has no imaginary frequencies, which helped to confirm that the structure of the compound deduced following geometry optimization corresponds to an energy minimum. There are 126 vibrations.

JRS

Table 1. Optimized geometric parameters of NKA

Bond length/Å		Bond Angle/°		Dihedral angle/°	
C_2—C_1	1.3345	A (2,1,3)	115.1145	D (3,2,1,4)	−179.9956
H_3—C_1	1.0763	A (2,1,4)	130.608	D (3,1,2,5)	−0.2195
C_4—C_1	1.5038	A (1,2,5)	121.5463	D (3,1,2,6)	179.971
C_5—C_2	1.5117	A (1,2,6)	125.0613	D (2,1,4,7)	63.1608
C_6—C_2	1.48	A (1,4,7)	111.4516	D (2,1,4,8)	−56.2184
H_7—C_4	1.0818	A (1,4,8)	111.7525	D (2,1,4,9)	−176.7431
H_8—C_4	1.0809	A (1,4,9)	109.854	D (1,2,5,10)	0.4247
H_9—C_4	1.0819	A (2,5,10)	110.5536	D (1,2,5,11)	120.98.95
H_{10}—C_5	1.0817	A (2,5,11)	111.1793	D (1,2,5,12)	−120.1475
H_{11}—C_5	1.0832	A (2,5,12)	111.1698	D (5,2,6,13)	−2.182
H_{12}—C_5	1.0831	A (2,6,13)	121.9959	D (5,2,6,14)	178.3485
O_{13}—C_6	1.2202	A (2,6,14)	115.3003	D (13,6,14,15)	7.7174
O_{14}—C_6	1.3451	A (6,14,15)	128.2099	D (6,14,15,16)	161.7069
C_{15}—O_{14}	1.4806	A (14,15,16)	102.3274	D (6,14,15,1)	43.2265
C_{16}—C_{15}	1.5269	A (14,15,17)	112.2741	D (14,15,17,18)	55.6608
C_{17}—C_{15}	1.5257	A (15,17,18)	109.4978	D (14,15,17,19)	−64.9803
H_{18}—C_{17}	1.083	A (15,17,19)	113.1008	D (14,15,17,20)	173.5673
H_{19}—C_{17}	1.0763	A (15,17,20)	108.5772	D (14,15,17,21)	−62.0517
H_{20}—C_{17}	1.0817	A (15,16,21)	108.5772	D (14,15,16,22)	57.3854
H_{21}—C_{16}	1.0816	A (15,16,22)	110.553	D (14,15,16,23)	177.6154
H_{22}—C_{16}	1.0818	A (15,16,23)	110.1168	D (6,14,15,24)	−83.2023
H_{23}—C_{16}	1.0794	A (14,15,24)	106.8276	D (14,15,24,25)	−167.6844
C_{24}—C_{15}	1.5368	A (15,24,25)	106.3775	D (9,15,24,25,26)	−139.6282
O_{25}—C_{24}	1.468	A (24,25,26)	109.9198	D (24,25,26,27)	6.6747
C_{26}—O_{25}	1.3675	A (25,26,27)	111.786	D (25,26,27,28)	1.4988
C_{27}—C_{26}	1.3928	A (26,27,28)	109.0707	D (24,25,26,29)	−173.3037
C_{28}—C_{27}	1.5112	A (25,26,29)	124.6695	D (27,26,29,30)	0.0691
C_{29}—C_{26}	1.3724	A (26,29,30)	115.9724	D (26,29,30,31)	−0.074
C_{30}—C_{29}	1.3871	A (29,30,31)	122.8199	D (929,30,31,32)	0.1622
C_{31}—C_{30}	1.3924	A (30,31,32)	118.8685	D (26,29,30,33)	−179.8942
C_{32}—C_{31}	1.404	A (29,30,33)	117.3829	D (31,30,33,34)	0.0585
O_{33}—C_{30}	1.3722	A (30,33,34)	124.6352	D (30,33,34,35)	0.002
C_{34}—O_{33}	1.3803	A (33,34,35)	115.4361	D (33,34,35,36)	−0.0409
C_{35}—C_{34}	1.456	A (34,35,36)	121.1093	D (26,27,28,37)	112.2993
C_{36}—C_{35}	1.3379	A (27,28,37)	111.9328	D (26,27,28,38)	−127.0319
H_{37}—C_{28}	1.078	A (27,28,38)	112.5962	D (26,27,32,39)	−179.6675
H_{38}—C_{28}	1.0821	A (27,32,39)	121.0774	D (34,35,36,40)	179.9923
H_{39}—C_{32}	1.0738	A (35,36,40)	120.0909	D (33,34,35,41)	179.9472
H_{40}—C_{36}	1.0734	A (34,35,41)	115.9599	D (30,33,34,42)	−179.9922
H_{41}—C_{35}	1.0688	A (33,34,42)	118.6683	D (27,26,29,43)	−179.8069
O_{42}—C_{34}	1.2071	A (26,29,43)	122.9816	D (26,25,24,44)	105.6207
H_{43}—C_{29}	1.0684	A (25,24,44)	106.46978		
H_{44}—C_{24}	1.0802				

Comparison between calculated and experimental spectra

The wavenumber values computed at the Hartree–Fock level contain known systematic errors due to the neglect of electron correlation and harmonic approximation, resulting in an overestimate of about 10–12%. Therefore, it is usual to scale wavenumbers predicted at the Hartree–Fock level by an empirical factor of 0.8929 to correlate with the experimental values of vibrational wavenumbers.

C–H vibrations

The asymmetric C–H stretching wavenumber of CH_3 is expected around 2962 cm^{-1} and the symmetric one around 2872 cm^{-1}.[16,17] In NKA there are four CH_3 groups labeled I,

Table 2. Calculated vibrational wavenumbers measured infrared and Raman band positions (cm^{-1}) and assignments for NKA

HF/6–31 G scaled wavenumbers cm^{-1}	Experimental		IR intensity		Raman activity		Depolarization ratio	Force constant	Assignment
	FTIR cm^{-1}	Raman cm^{-1}	Absolute	Relative	Absolute	Relative			
	3442 w								C═O overtone
3069		3086 w	1.20	0.19	75.51	28.15	0.29	7.63	Aromatic C–H stretch
3064	3050 sh	3052 w	0.79	0.12	154.011	57.42	0.25	7.66	
2992	2989 m	3000 w	4.92	0.79	23.79	8.87	0.64	7.26	CH_3 asym. stretch of IV
2966	2969 w		26.78	3.00	53.95	20.12	0.70	7.16	CH_3 asym. stretch of III
2939	2944 m	2943	1.14	0.00	77.47	28.89	0.73	7.02	CH_3 asym. stretch of I
2930			37.29	5.98	74.79	27.89	0.72	6.98	
2914	2910 sh	2912 sh	22.49	3.61	68.36	35.49	0.74	6.90	CH_3 asym. stretch of II
2878			21.94	3.52	214.72	80.06	0.04	6.36	CH_3 sym. stretch of III
2872			21.11	3.55	22.39	8.31	0.13	6.33	CH_3 sym. stretch of IV
2869	2864 sh	2867 br sh	20.56	3.29	122.89	45.58	0.05	6.31	CH_3 sym. stretch of I
2860	2856 sh	2867 w	29.16	4.78	111.98	41.75	0.01	6.26	CH_3 sym. stretch of II
1722	1717 vvs	1731 m	623.69	100.0	128.37	47.86	0.41	23.03	C_{34}═O_{42} stretch
1713		1712 s	136.70	21.92	123.88	46.19	0.28	16.59	C_6═O_{13} stretch
1636	1627 vs	1628 s	30.97	4.97	156.91	58.5	0.24	13.85	Ring stretch. + aromatic CH bend
1579	1571 vs	1571 vvs	72.77	11.67	266.21	99.26	0.38	16.09	Ring stretch
1483	1487 vs	1485	40.30	6.46	11.54	4.30	0.59	1.97	CH_3 asym. bend of III and IV
1451	1445 s	1442 w	23.14	3.71	9.89	3.69	0.66	1.67	CH_3 asym. bend of I and II
1394	1396 s	1395 s	49.24	7.89	29.90	11.15	0.43	2.26	CH_3 sym. bend.
1389	1385 s		29.93	4.6	26.46	9.32	0.42	2.79	Aromatic CH bend
1350	1367 s	1368 vvs	48.39	7.76	268.20	100.00	0.28	4.37	Ring vibration
1273	1270 vs	1259 w	320.03	51.31	10.33	3.85	0.28	3.67	C–C–O sym. stretch and C_1–H_3 bend
1249	1255 sh	1259 w	7.86	1.25	4.39	1.64	0.35	1.95	Aromatic CH bend
1219	1229 vs	1221 vw	169.00	27.10	11.44	4.27	0.49	4.42	Aromatic CH bend
1185	1183 sh	1183 s	2.71	0.43	69.71	25.99	0.31	2.61	Ring breathing aromatic CH bend
1158	1158 sh	1153 s	36.13	5.79	22.18	8.27	0.34	2.21	Ring breathing
1123	1127 vvs	1134 sh	363.00	58.20	4.29	1.60	0.17	2.36	Aromatic CH and C–O bend
1084	1085 m	1084 w	5.63	0.90	1.76	0.66	0.31	1.31	CH bend
1058	1043 m	1043 vw	70.43	11.29	18.13	6.76	0.36	3.00	Aromatic CH bend
1043	1004 m	1007 vw	13.35	2.14	2.69	1.00	0.72	2.10	CH bend
970	977 s	981 vw	135.12	21.66	6.96	2.49	0.52	2.74	C_{24}–O_{25}, C_{24}–H_{44} and C_{29}–H_{43} bend
947	929 m	917 w	32.99	5.29	1.73	0.65	0.69	0.98	Aromatic CH bend
814	819 s	811 w	40.16	6.44	18.87	7.04	0.30	2.46	C_6–O_{14} bend and $C_{24,29}$–$H_{43,44}$ bend
767	755 w	770 m	29.51	4.73	9.75	3.64	0.75	1.89	C_{30}–C_{31} and C_{34}–C_{35} bend

(*continued overleaf*)

Table 2. (*Continued*).

HF/6–31 G scaled wavenumbers cm^{-1}	Experimental		IR intensity		Raman activity		Depolarization ratio	Force constant	Assignment
	FTIR cm^{-1}	Raman cm^{-1}	Absolute	Relative	Absolute	Relative			
744	720 m	721 w	19.11	3.06	13.28	4.95	0.19	2.04	C_6–O_{14} and C_{32}–H_{39} bend
642	610 w		8.30	1.33	4.45	1.66	0.43	1.23	CH bend
587	561 w	567 w	5.95	0.95	3.48	1.29	0.40	1.18	In-plane skeletal deform.
490	496 w	497 w	14.19	2.28	5.76	2.15	0.67	0.77	C–C and C–H bend
422	418 w	415 w	5.33	0.85	8.66	3.23	0.40	0.67	CH bend
267	275 w		5.37	0.86	2.79	1.04	0.49	0.22	

Table 3. CH bond lengths and HCH angles of CH_3 groups

CH_3 group No.	CH bond length/Å		HCH bond angle/°	
I	C_4—H_7	1.0818	A (7,4,8)	106.7717
	C_4—H_8	1.0809	A (7,4,9)	108.3476
	C_4—H_9	1.0819	A (8,4,9)	108.5312
II	C_5—H_{10}	1.0817	A (10,5,11)	108.4899
	C_5—H_{11}	1.0832	A (10,5,12)	108.5011
	C_5—H_{12}	1.0831	A (11,5,12)	106.8136
III	C_{16}—H_{21}	1.0816	A (21,16,22)	108.4129
	C_{16}—H_{22}	1.0818	A (21,16,23)	108.3568
	C_{16}—H_{23}	1.0794	A (22,16,23)	108.7799
IV	C_{17}—H_{18}	1.083	A (18,17,19)	108.1165
	C_{17}—H_{19}	1.0763	A (18,17,20)	108.1716
	C_{17}—H_{27}	1.0817	A (19,17,20)	109.2653

Table 4. Short (C—) H···O distances

CH_3 group No.	Contact	(C—) H···O/Å
I	H_7···O_{14}	2.629
	H_8···O_{14}	2.549
	H_9···O_{14}	3.858
II	H10···O13	3.819
	H11···O13	2.718
	H12···O13	2.712
III	H21···O14	2.509
	H22···O14	2.530
	H23···O14	3.079
IV	H18···O13	3.263
	H19···O13	2.423
	H18···O14	2.708
	H19···O14	2.829

II, III and IV (Fig. 1). In the ester part groups I and II are attached to C_1 and C_2, respectively, and groups III and IV are attached to C_{15}. Normal-mode calculations were used in the assignment of vibrational modes of the different CH_3 groups. The asymmetric stretch of CH_3 group IV appears as a shoulder at 2989 cm^{-1} in IR and as a weak band at 3000 cm^{-1} in Raman, whereas the corresponding vibration of CH_3 group III is observed at 2969 cm^{-1} in IR. Although these two CH_3 groups are structurally similar, their asymmetric stretching wavenumbers are different, which can be attributed to the difference in their environment. From the distance matrix of the optimized geometry of NKA, the C—H···O distances were evaluated to assess the effect of intramolecular hydrogen bonding in methyl groups. The different CH distances and HCH angles (Table 3) and the short C—H···O distances (Table 4) of the methyl groups indicate that the shift of the asymmetric stretching wavenumber in CH_3 groups III and IV is due to C—H···O hydrogen bonding.[18] It has recently been reported that the spectroscopic behavior of C—H···O hydrogen bonds is generally opposite to that of typical (e.g. O—H···O and N—H···O) hydrogen bonds and the C–H stretching wavenumber is blue-shifted and the infrared band intensity decreases on hydrogen bonding.[19] The shortest C—H···O distance for CH_3 group IV is 2.423 Å, whereas the corresponding value for CH_3 group III is 2.509 Å. These values clearly suggest a stronger influence of blue-shifting hydrogen bonds for CH_3 group IV than that of CH_3 group III, which resulted in higher ν_{as} values for group IV. The blue-shifting hydrogen bond may be understood on the basis of the dynamic properties of the donor group. The interaction of the external electric field created by the acceptor atom with the permanent and induced dipole derivatives of the X—H bond exert force on the H···O bond. When the field and dipole derivative are anti-parallel, which is the case with C—H···O, the bond shortens. This results in blue-shifting of the C–H stretching wavenumber and a decrease in intensity. Hence this mechanism is responsible for shifting the asymmetric stretching of CH_3 groups III and IV the shift being greater for group IV.

The asymmetric stretching vibrational wavenumbers of groups I and II are found to be considerably lowered owing to the influence of hyperconjugation.[20] The C—H···O distance of these groups also indicates the presence of C—H···O hydrogen bonding. The hyperconjugation[5] and blue-shifting

due to the C—H···O hydrogen bond are competing in effect. The impact of hyperconjugation on the CH_3 asymmetric stretching wavenumber of CH_3 groups I and II is more pronounced. From the spectra and computation it is evident that CH_3 group I with the shorter C—H···O distance[17] has a higher asymmetric CH stretching wavenumber than CH_3 group II. The CH_3 asymmetric stretching vibration of group I is observed at 2944 cm^{-1} in IR and 2943 cm^{-1} in Raman, whereas the corresponding mode of CH_3 group II is observed as a shoulder at 2910 cm^{-1} in IR and as a shoulder at 2912 cm^{-1} in Raman.

The band at 2864 cm^{-1} in IR and the broad shoulder at 2867 cm^{-1} in Raman are expected to arise from the symmetric stretching of the four CH_3 groups. Although the calculated symmetric stretching wavenumbers arising from different CH_3 groups show slightly different wavenumber values, they could not be separated in the spectra.

The asymmetric bending vibration of methyl groups normally appears around 1460 cm^{-1} and the symmetric one around 1375 cm^{-1}. A very intense IR band at 1487 cm^{-1} and a weak Raman band at 1485 cm^{-1} are assigned to the asymmetric bending vibration of CH_3 groups III and IV. The corresponding bending modes of I and II are observed at 1445 cm^{-1} in IR and 1442 cm^{-1} in Raman. Lowering of the CH bending vibration of CH_3 groups I and II further supports the presence of hyperconjugation. The symmetric bending vibration of methyl groups is observed at 1396 cm^{-1} in Raman and at 1395 cm^{-1} in IR.

Aromatic C–H stretching vibrations occur at values between 3000 and 3100 cm^{-1}.[21] In NKA, two weak bands at 3086 and 3052 cm^{-1} in Raman and a shoulder at 3050 cm^{-1} in IR can be assigned to aromatic C–H stretching modes. The normal mode analysis also supports these assignments.

C–O vibrations

Esters are characterized by two strong IR absorptions, one due to the C=O stretching vibration in the range 1750–1735 cm^{-1} and the other due to C–O stretching vibrations near 1200 cm^{-1}. The unstrained, six-membered cyclic ester,[22] δ-lactone, absorbs at about the same wavenumber as a non-cyclic ester. Generally, C=O stretching intensities are relatively higher in IR than in Raman. The conjugated ester part —C=C—C—O— gives an intense IR band at 1720 cm^{-1}.[23] In NKA the C=O bond in the ester part is conjugated with C_1=C_2 and C=O in the lactone part is conjugated with C_{35}=C_{36} and C_{30}=C_{31} double bonds. The increase in single bond character due to conjugation lowers the wavenumber of the carbonyl and double bond vibrations. In the present study, the carbonyl vibrational wavenumbers in the ester part (C_6=O_{13}) and in the lactone part (C_{34}=O_{42}) have been lowered to different extents owing to conjugation, resulting in two closely spaced bands with slightly different wavenumbers, calculated at 1722 and 1713 cm^{-1}, respectively. In the Raman spectrum, bands resulting from ester and lactone carbonyl vibrations are observed as a medium-intensity band at 1712 cm^{-1} and an intense band at 1731 cm^{-1}, respectively. The C=O stretching vibration which normally appears as a sharp, intense band in IR is broadened in NKA around 1717 cm^{-1} owing to overlap of the ester and lactone carbonyl vibrations. From the splitting observed in the Raman spectrum and the computed carbonyl wavenumbers, it can be inferred that the effect of conjugation is more pronounced in the ester part than in the lactone part.

The strongly intense bands at 1270 cm^{-1} in IR and a shoulder at 1270 cm^{-1} in the Raman spectrum are assigned to stretching of C_2—C_6 and C_6—O_{14} attached to the carbonyl carbon ('C–C–O' symmetric stretch). The corresponding band obtained by normal-mode analysis of this band is 1273 cm^{-1}. The observed medium-intensity band at 3442 cm^{-1} is probably an overtone of the C=O stretching vibration.

Ring vibrations

Owing to conjugation of C=O with C_{35}=C_{36} and C_{30}=C_{31} double bonds, the electron density distribution in the lactone ring is influenced,[21] which results in weakening of the C_{35}=C_{36} bond and strengthening of the C_{34}—C_{35} bond. This is apparent from slightly lowered wavenumbers for ring vibrations involving C_{35}—C_{36}. We calculated the vibrational wavenumbers of the lactone part separately, which was useful in the assignment of the ring vibrations of NKA (Table 5). Normal-mode analysis from *ab initio* vibrational computations[15] showed that breathing modes of the condensed ring are coupled with aromatic CH deformation modes. A number of vibrational modes characteristic of the lactone ring in NKA have been identified for the first time: the sharp, intense band at 1571 cm^{-1} in Raman and IR (ν_{49} of the lactone ring), the very strong Raman band at 1368 cm^{-1} and the medium-intensity IR band at 1367 cm^{-1} (ν_{42} of the lactone ring), the medium-intensity band at 1183 cm^{-1} in Raman and a shoulder at 1183 cm^{-1} in IR (ν_{36} of the lactone ring) and the strong band at 1153 cm^{-1} in Raman and the shoulder at 1158 cm^{-1} in IR (ν_{34} of the lactone ring).

SERS spectral analysis

The SERS spectrum of NKA is dominated by five strong lines at wavenumbers 1630, 1585, 1390, 1190 and 1160 cm^{-1} (Fig. 5). The wavenumbers of surface-enhanced Raman lines (2000–800 cm^{-1}) and their vibrational assignments are given in Table 6. From these assignments, it appears that the intense lines in the SERS spectrum draw their intensity from in-plane ring vibrations of the lactone moiety. This indicates that the NKA molecule is adsorbed on the metal surface through lactone ring π electrons. Moreover, the very intense band at 1712 cm^{-1} in the NIR-FT Raman spectrum assigned to the carbonyl stretching vibration (C_6=O_{13}) of the ester part of the molecule is not observed in the SERS spectrum and this also supports the above assumption

Table 5. Calculated vibrational wavenumbers (cm^{-1}) of lactone part

Species	Mode	ν_{cal} / cm^{-1}	ν_{scaled} / cm^{-1}	IR intensity	Raman activity	Depolarization ratio
A'	ν_5	246	219	0.26	0.46	0.63
	ν_8	393	351	6.57	14.49	0.35
	ν_9	427	381	9.43	4.6	0.19
	ν_{12}	541	483	5.48	3.66	0.23
	ν_{13}	590	527	13.10	4.25	0.67
	ν_{14}	667	596	7.9	2.29	0.46
	ν_{16}	778	695	28.34	1.32	0.59
	ν_{18}	791	706	2.84	3.76	0.37
	ν_{19}	828	739	1.42	11.67	0.20
	ν_{21}	876	782	5.95	25.03	0.12
	ν_{23}	930	830	8.83	1.40	0.13
	ν_{25}	1004	896	5.49	13.11	0.37
	ν_{27}	1028	918	52.87	6.57	0.17
	ν_{29}	1080	964	45.14	6.19	0.73
	ν_{31}	1182	1055	54.51	11.38	0.37
	ν_{33}	1255	1121	250.51	5.87	0.16
	ν_{34}	1293	1155	46.86	20.44	0.27
	ν_{36}	1324	1182	23.86	63.34	0.28
	ν_{37}	1347	1203	201.04	5.68	0.75
	ν_{38}	1376	1229	11.17	55.58	0.44
	ν_{40}	1399	1249	7.63	8.84	0.36
	ν_{41}	1434	1280	3.30	13.17	0.19
	ν_{42}	1476	1318	68.19	227.88	0.27
	ν_{43}	1520	1357	0.25	19.19	0.35
	ν_{44}	1555	1388	45.49	2707	0.34
	ν_{45}	1609	1437	21.58	3.96	0.32
	ν_{46}	1651	1474	29.25	20.07	0.74
	ν_{47}	1660	1482	59.12	14.85	0.37
	ν_{48}	1684	1504	2.04	24.82	0.53
	ν_{49}	1765	1576	140.55	267.67	0.41
	ν_{50}	1817	1622	101.67	10.64	0.57
	ν_{51}	1839	1642	283.18	272.46	0.29
	ν_{52}	1926	1720	827.28	156.5	0.31
	ν_{53}	3216	2872	26.53	145.64	0.16
	ν_{55}	3275	2924	63.86	192.51	0.09
	ν_{57}	3362	3002	4.91	40.07	0.31
	ν_{58}	3371	3010	12.50	95.02	0.42
	ν_{59}	3431	3064	0.83	139.11	0.24
A''	ν_1	24	21	3.23	0.09	0.75
	ν_2	87	78	0.66	0.33	0.75
	ν_3	144	129	6.36	1.14	0.75
	ν_4	193	172	4.21	0.11	0.75
	ν_6	307	274	12.69	2.56	0.75
	ν_7	364	325	1.98	0.12	0.75
	ν_{10}	475	424	1.8	6.47	0.75
	ν_{11}	520	464	2.75	0.88	0.75
	ν_{15}	731	653	0.69	4.82	0.75
	ν_{17}	780	696	0.43	2.69	0.75
	ν_{20}	857	765	28.3	8.88	0.75
	ν_{22}	917	819	0.025	0.49	0.75
	ν_{24}	945	844	70.18	2.74	0.75
	ν_{26}	1010	902	22.77	1.54	0.75
	ν_{28}	1067	953	29.63	1.92	0.75
	ν_{30}	1173	1047	0.00	10.67	0.75
	ν_{32}	1208	1078	3.29	0.49	0.75
	ν_{35}	1323	1181	0.85	10.97	0.75
	ν_{39}	1380	1232	0.25	8.89	0.75
	ν_{54}	3253	2905	12.07	82.88	0.75
	ν_{56}	3334	2977	28.35	122.03	0.75

Assuming a C_s local point group for the planar lactone ring, it is very likely that the strongest SERS line arise from the vibrational modes of A' symmetry. These modes involve the diagonal tensor components, α_{zz} (α_{xx}, α_{yy}). On this basis, the orientation of the lactone plane with respect to the silver surface can be inferred using the so-called SERS selection rules.[24–27] In brief, these rules state that for a planar molecular system perpendicular to the surface, enhanced Raman lines are expected for totally symmetric in-plane modes, which derived their intensity from the α_{zz} tensor component, where z is the local axis normal to the surface. Since, in the present case, A' vibrations corresponding to in-plane ring stretching and ring breathing vibrations of the lactone ring are the most intense, it can be concluded that the lactone plane is directed normal to the metal surface. Finally, it should be noted that the carbonyl stretching of the lactone ring (C_{34}═O_{42}) appears only as a weak band at 1720 cm^{-1} in the SERS spectrum. The weakening of this carbonyl stretching vibration indicates that the lactone C═O is not in direct interaction with the silver surface.

Table 6. Band positions and assignments of SERS and normal Raman (NR) spectra of NKA (2000–800 cm^{-1})

SERS/cm^{-1}	NR cm^{-1}	Assignment
1720 vw	1731 m	C_{34}═O_{42}
1630 s	1628 s	Ring stretch
1585 vs	1571 vvs	Ring stretch
1460 w	1442 w	CH_3 asym. bend
1400 w	1396 s	CH_3 sym. bend
1390 s	1368 vvs	Ring vib.
1320 w	1325 w	Aromatic CH bend
1275 m	1259 w	C–C–O stretch (ester part)
1190 s	1183 s	Ring breathing, aromatic CH bend
1160 s	1153 s	Ring breathing
1140 m	1134 sh	Aromatic CH bend

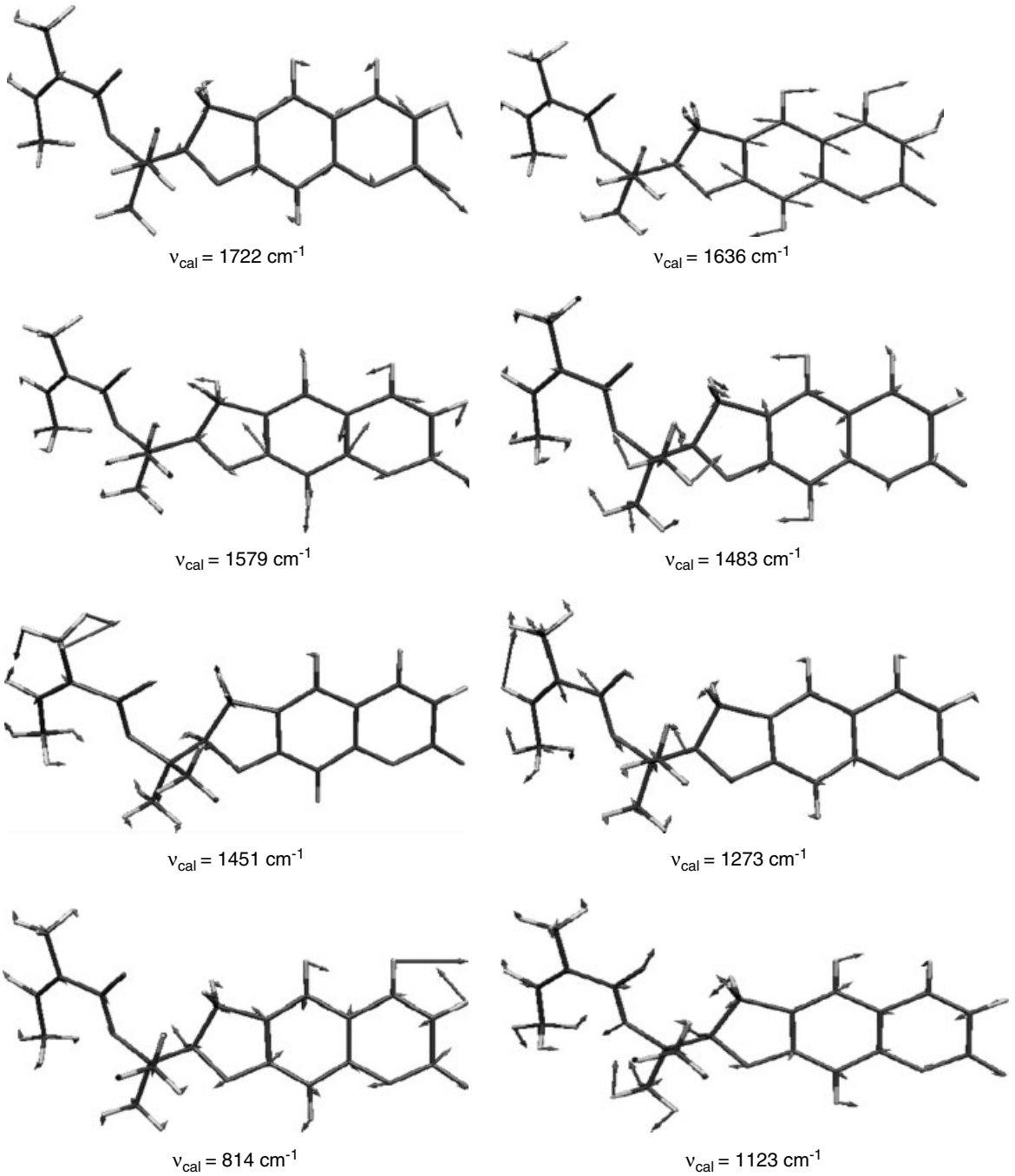

Figure 5. Selected normal modes of vibrations of nodakenetin angelate from Hartee–Fock calculation.

CONCLUSION

This vibrational spectral analysis of NKA reveals that the four methyl groups of NKA show different spectral characteristics while the methyl group IV exhibits a blue shift for the methyl asymmetric stretching wavenumber due to intramolecular C—H···O interaction. It is found that the carbonyl stretching wavenumber has been lowered for C═O groups belonging to both the lactone and ester parts owing to the increase in single bond character that occurs due to the conjugation with the neighboring C═C bonds. The electron density distribution of lactone ring is disturbed owing to the conjugation with the carbonyl group, which is found to change the spectral modes of the lactone ring. SERS spectral analysis reveals that the lactone plane is directed normal to the silver surface and the C═O group is not in direct interaction with the metal surface.

Acknowledgements

J.P.A. thanks the University Grants Commission, Government of India, for the award of a teacher fellowship under FIP. O.F.N. thanks the Danish Natural Science Research Council for financial support during this project. The support provided by Dr K. S. Viswanathan, Materials Chemistry Division, IGCAR, Kalpakkam, India, in the computational work is gratefully acknowledged.

REFERENCES

1. Tu AT. *Raman Spectroscopy in Biology*. Wiley: New York, 1982.
2. Carey PR. *Biochemical Applications of Raman and Resonance Raman Spectroscopies*. Academic Press: London, 1982.
3. Clark RJH, Hester RE (eds). *Spectroscopy of Biological Systems. Advances in Spectroscopy*, vol. 13. Wiley: Chichester, 1986.
4. Faurskov Nielsen O. In *Handbook of Raman Spectroscopy*, Lewis IR, Edwards HGM (eds). Marcel Dekker: New York, 2001; 393.
5. Abraham JP, Joe IH, George V, Faurskov Nielsen O, Jayakumar VS. *Spectrochim. Acta, Part A* 2003; **59**: 193.
6. Vogel E, Gbureck A, Kiefer W. *J. Mol. Struct.* 2000; **550–551**: 177.
7. Zhu W-L, Puah CM, Tan X-J, Jiang H-L, Chen K-X, Ji R-Y. *J. Mol. Struct. (Theochem)* 2000; **528**: 193.
8. Binoy J, Abraham JP, Joe IH, Jayakumar VS, Pettit GR, Faurskov Nielsen O. *J. Raman Spectrosc.* 2004; **35**: 939.
9. Sajan D, Binoy J, Pradeep B, Venkata Krishna K, Kartha VB, Joe IH, Jayakumar VS. *Spectrochim Acta, Part A* 2004; **60**: 173.
10. Mukherjee PK, Constance L. *Umbelliferae (Apiaceae) of India*. Oxford and IBH Publishing Company Pvt Ltd New Delhi, 1993; 243.
11. Saradamma L, Nair CPR, Bhatt AV, Rajasekaran S, Lakshmi N, Nair VV. *All India Co-ordinated Research Project on Ethnobotany. Technical Report (AICRP) Phase II*. Ministry of Environment and Forests (MOEF), Govt of India, New Delhi, 1990; 243 1987–90; 243.
12. Samuelsson G,. *Drugs of Natural Origin. A Text Book of Pharmacognosy*. Swedish Pharmaceutical Press: Stockholm, 1992; 97.
13. Nielsen E, Larsen PK, Lemmich J. *Acta Chem. Scand.* 1970; **24**: 2863.
14. *Dictionary of Natural Products* (1st edn), vol. 2D–F. Chapman and Hall: London, 1994; 1522.
15. Frisch MJ, Trucks GW, Schelegal HB, Scuseria GE, Robb MA, Cheeseman JR, Zakrzewski VG, Montgomery Jr JA, Stratmann RE, Burant JC, Dapprich S, Millam JM, Daniels AD, Kudin KN, Strain MC, Farkas O, Tomasi J, Barone V, Cossi M, Cammi R, Mennucci B, Pomelli C, Adamo C, Clifford S, Ochterski J, Peterson GA, Ayala PY, Cui Q, Morokuma K, Malick DK, Rabuck AD, Raghavachari K, Foreman JB, Cioslowski J, Ortiz JV, Baboul AG, Stefanov BB, Liu G, Liashenko A, Piskorz P, Komaromi I, Gomperts R, Martin RL, Fox DJ, Keith T, Al-Laham MA, Peng CY, Nanayakkara A, Challacombe M, Gill PMW, Johnson B, Chen W, Wong MW, Andres JL, Gonzalez C, Head-Gordon M, Replogle ES, Pople JA. *Gaussian 98*. Gaussian: Pittsburgh, PA, 1998.
16. Silverstein RM, Bassler GC, Morrill TC. *Spectrometric Identification of Organic Compounds* (5th edn). Wiley: New York, 1991.
17. Bellamy LJ. *The Infrared Spectra of Complex Molecules*. Wiley: Chichester, 1975.
18. Taylor R, Kennard O. *J. Am. Chem. Soc.* 1982; **104**: 5063.
19. Qian W, Krimm S. *J. Phys. Chem. A* 2002; **106**: 6628.
20. Morrison RT, Boyd RN. *Organic Chemistry*. Prentice Hall: Englewood Cliffs, NJ, 1989.
21. Smith B. *Infrared Spectral Interpretation*. CRC Press: Boca Raton, FL, 1999.
22 Pavia DL, Lampman GM, Kriz G. *Introduction to Spectroscopy, a Guide for Students of Organic Chemistry* (3rd edn). Hartcourt College Publishers: Orlando, FL, 2001.
23. Dollish FR, Fateley WG, Bentley FF. *Characteristic Raman Frequencies of Organic Compounds*. J Wiley: New York, 1997.
24. Moskovits M. *J. Chem. Phys.* 1982; **77**: 4408.
25. Moskovits M, Dilella DP. *Chem. Phys. Lett.* 1980; **73**: 500.
26. Moskovits M, Suh JS. *J. Phys. Chem.* 1984; **88**: 1293.
27. Allen CS, Vanduyne RP. *Chem. Phys. Lett.* 1979; **63**: 455.